Geophysical Journal International

Geophys. J. Int. (2019) **216,** 598–608
Advance Access publication 2018 October 25
GJI Geomagnetism, rock magnetism and paleomagnetism

doi: 10.1093/gji/ggy446

Primary pseudo-single and single-domain magnetite inclusions in quartzite cobbles of the Jack Hills (Western Australia): implications for the Hadean geodynamo

Richard K. Bono,[1,2] John A. Tarduno[1,3] and Rory D. Cottrell[1]

[1] *Department of Earth and Environmental Science, University of Rochester, Rochester, NY, USA 14627. E-mail: richard.bono@rochester.edu*
[2] *Geomagnetism Laboratory, Earth and Ocean Sciences, University of Liverpool, Liverpool, UK L69 7ZE*
[3] *Department of Physics and Astronomy, University of Rochester, Rochester, NY, USA 14627*

Accepted 2018 October 24. Received 2018 October 19; in original form 2018 July 31

SUMMARY

Zircons of the Jack Hills of Western Australia are the oldest known terrestrial minerals and as such they hold potential for recording Earth's oldest geomagnetic field. To preserve records of the most ancient magnetic field, the zircon host rocks must not have been heated to temperatures that resulted in a complete remagnetization. To test this hypothesis, magnetic minerals having very high unblocking temperatures must be present in the host rocks and capable of retaining magnetizations on billion-year timescales. Here, we use scanning electron microscopy analyses and transmission electron microscopy characterization of focused ion beam lift outs to document for the first time through direct imaging the presence of pseudo-single (PSD) to single-domain (SD) magnetite inclusions in Jack Hills quartzite cobbles. We further use focused ion milling to document the 3-D detrital morphology of an inclusion and micromagnetic modelling that suggest a single vortex magnetization. These results, together with recent advances in our understanding of the blocking temperatures and relaxation times of PSD grains, indicate that the Jack Hills host rocks contain magnetic inclusions capable of recording magnetizations as old as the age of the conglomerate (ca. 3 billion years old). These new results confirm that magnetic directions observed retained at high unblocking temperatures (500–580 °C) in these rocks identified in two independent laboratory analyses are carried by PSD/SD magnetite. The lack of an overprint direction recorded at these high temperatures excludes pervasive thermal and/or chemical remagnetization and indicates that the oldest zircons from the Jack Hills are potential recorders of the Hadean geodynamo.

Key words: Palaeomagnetism; Australia; Rock and mineral magnetism; Image processing; Numerical modelling.

1 INTRODUCTION

Single silicate crystals are attractive targets for probing the nature of the past geomagnetic field because they often contain minute magnetic minerals with ideal recording properties (Cottrell & Tarduno 1999, 2000; Feinberg *et al.* 2005; Dunlop 2002). The single crystal palaeointensity (SCP) method was developed to explore this record (Cottrell & Tarduno 1999; Tarduno *et al. 2006,* 2009). Over the last 20 yr, this technique has been applied to understand the geomagnetic field during times of reversals and superchrons (Tarduno & Smirnov 2001; Tarduno *et al.* 2002; Tarduno & Cottrell 2005; Cottrell *et al.* 2008), as well as the field of the Precambrian (Smirnov *et al.* 2003; Tarduno *et al.* 2007; Bono & Tarduno 2015). A particular focus of the latter studies has been the long-term nature of the magnetic shielding of Earth from the solar wind and its relationship with planetary habitability (Tarduno *et al.* 2014).

SCP data, together with select whole rock studies where the magnetizations are likely dominated by silicate hosted inclusions (e.g. Selkin *et al.* 2008; Muxworth *et al.* 2013) form the basis for our current understanding of the strength of the field during Archean times. These data provide a consistent picture of a robust field, similar in strength to the modern one. The oldest record of field strength from intact rock sequences comes from SCP studies of the Palaeoarchean (3.4–3.45 billion years old) Nondweni and Barberton Greenstone Belts of South Africa Tarduno *et al.* (2010). To date, all older extant rocks have been observed to have metamorphic grades of amphibolite facies (or higher) and thus incompatible with the preservation of primary magnetic signals.

A source of even older records of the magnetic field are crystals found within younger sedimentary rocks that may have escaped high-grade metamorphism. The oldest known terrestrial crystals are zircons found in mature siliciclastic sediments of the Jack Hills of

© The Author(s) 2018. Published by Oxford University Press on behalf of The Royal Astronomical Society. This is an Open Access article distributed under the terms of the Creative Commons Attribution License (http://creativecommons.org/licenses/by/4.0/), which permits unrestricted reuse, distribution, and reproduction in any medium, provided the original work is properly cited.

Downloaded from https://academic.oup.com/gji/article-abstract/216/1/598/5144769 by Univ of Rochester Library user on 23 November 2018

Western Australia, especially at a location known as the Discovery site (e.g. Wilde *et al.* 2001). Tarduno *et al.* (2015) presented the first magnetic records from zircons, which were collected at the Discovery site. These analyses indicate the presence of a magnetic field extending into the Hadean Eon (ca. 4.2 billion years ago).

As in the case of extant rocks, a pre-requisite for SCP studies of zircons is that the host sediment has escaped remagnetization. The Jack Hills sediments are in the greenschist facies; detailed thermometry on monazite–xenotime grains suggest metamorphic temperatures of 420–475 °C (Rasmussen *et al.* 2011). These temperatures are below the those required to reset a magnetization carried by single-domain (SD) or small pseudo-single-domain (PSD) magnetite grains (∼470–530 °C, Dare *et al.* 2016). But, all rocks of the Jack Hills are expected to carry magnetic overprints at magnetic unblocking temperatures equivalent to and less than the peak metamorphic temperature. Magnetic field tests are essential to explore the fidelity of magnetizations at higher unblocking temperatures.

The first field test of the Jack Hills sediment magnetization was performed by Tarduno & Cottrell (2013) on cobble-sized quartzites within 1 km of the Discovery site. These cobbles are also of importance because of the remote possibility that they might harbour a piece of Hadean 'rock'. Although a Hadean rock fragment remains elusive, the magnetic data indicated a positive conglomerate test showing the absence of an overprint at the highest unblocking temperatures (550–580 °C) providing confidence that a primary magnetization could be held by Jack Hills rocks and zircons.

Subsequently, Dare *et al.* (2016) in the first study coupling scanning electron microscopy (SEM), energy dispersive X-ray spectroscopy (EDS) and electron microprobe (EMP) analyses with palaeomagnetic data on the Jack Hills rocks, documented the presence of detrital stochiometric magnetite. The Dare *et al.* (2016) study focused on relatively large grains (>1 to 10's of micrometres in size) from which compositional data could be obtained to constrain provenance. At these sizes, most magnetite grains should be in the multidomain (MD) state and their magnetizations could have relaxed in the ca. 3 billion years since deposition of the Jack Hills sediments. A common assumption in palaeomagnetism is if magnetic grains isolated at these grain sizes are present, smaller grains will also be present as part of the natural detrital grain size distribution. And these grains are predicted to be present from the magnetizations documented in the original (Tarduno & Cottrell 2013) and in independent analyses conducted in a second laboratory as part of an interlaboratory exchange experiment (in the palaeomagnetism laboratory of Lehigh University, reported in Dare *et al.* 2016).

A secondary reason for this investigation stems from the claim by Weiss *et al.* (2015) that the Jack Hills were pervasively remagnetized 1 billion years ago. Dare *et al.* (2016) noted that this claim is irrelevant to tests of the preservation of a primary magnetization by the Jack Hills sediments and their hosted zircons because the magnetizations reported by Weiss *et al.* (2015) were isolated at temperatures known to have been affected by the greenschist metamorphism (Rasmussen *et al.* 2011) and not higher temperatures where a primary magnetization could be retained. However, even at these low temperatures, the pervasive 1 Ga remagnetization proposed by Weiss *et al.* (2015) is highly problematic and bears on basic interpretations and resolution issues in palaeomagnetism.

For example, Weiss *et al.* (2015) called for this magnetization to have affected the Discovery site, but Bono *et al.* (2016) pointed out errors in their site locations and an inappropriate use of statistics. None of the samples collected by Weiss *et al.* (2015) which they link to the Discovery site yield 1 Ga overprint directions. Weiss *et al.* (2015) averaged disparate directions which are separated by 81°. This resulted in a nominal uncertainly that included the 1 Ga direction only because it is so large (70°). Hence, the overprint is not defined by data, but instead by an uncertainty. The cause of the 81° in the directions reported by Weiss *et al.* (2015, 2016) still remains unclear, but it could be related to orientation errors (Bono *et al.* 2016).

In samples irrefutably collected at the Discovery sites, Cottrell *et al.* (2016) found that the metamorphic mineral fuchsite recorded a magnetization distinct from the 1 Ga direction, but consistent with a ca. 2.6 Ga age defined by the peak metamorphism documented by Rasmussen *et al.* (2011) and apparent polar wander constraints (Smirnov *et al.* 2013). More recently, Bono *et al.* (2018) applied a new cluster analysis to a larger data set of magnetizations from the Jack Hills cobbles. Bono *et al.* (2018) found intermediate unblocking temperature component magnetizations that passed a fold test at the 90 per cent confidence level with those recorded by the Discovery site fuchsite, lending further support to a coincidence of greenschist metamorphism and overprinting. Importantly, Bono *et al.* (2018) also analysed cobble data reported by Weiss *et al.* (2015) and found no evidence for a 1 Ga magnetic direction.

Thus, a pervasive 1 Ga overprint (Weiss *et al.* 2015) is not present in available data from the Discovery site, and is not present in magnetic data from Tarduno & Cottrell (2013) or Weiss *et al.* (2015). Essentially, the magnetic data from cobbles from Tarduno & Cottrell (2013), Dare *et al.* (2016) and Weiss *et al.* (2015) are similar with the exception that the Weiss *et al.* (2015) data look unusually noisy, preventing clear isolation of the highest unblocking temperatures in most (but not all) samples (see Bono *et al.* 2018).

We note that in a recent review Evans (2018) omitted the following salient points: (i) the independent laboratory analyses of Rochester samples by Lehigh University; (ii) the internal inconsistency of the Weiss *et al.* (2015) results linked to the Discovery site; (iii) the challenges to the Weiss *et al.* (2015) data analysis and interpretation detailed in Bono *et al.* (2016); and (iv) the agreement in cobble results between Weiss *et al.* (2015), Tarduno & Cottrell (2013) and Dare *et al.* (2016) presented in Bono *et al.* (2018). Because of basic differences in standards for palaeomagnetic analysis (e.g. viable sample volume, see discussion in Dare *et al.* 2016) our attempts to engage B. Weiss in a sample exchange (in 2017 February) were unsuccessful. Given the fundamental differences in data analysis and interpretation, it is doubtful that additional remanence measurements will resolve any scientific debate. These differences in interpretation and data quality are best evaluated by readers through an exploration of data which are available at Earthref.org (Koppers *et al.* 2008).

Dare *et al.* (2016) offered several reasons why the Weiss *et al.* (2015) cobble data might be problematic. If submicrometre magnetite grains are present in the Jack Hills cobbles, they should hold high unblocking temperature magnetizations (e.g., Almeida *et al.* 2016). Thus, the absence/presence of these grains provides another means of evaluating the present conflicting interpretations of the Jack Hills magnetic data from quartzite cobbles: the interpretation of Weiss *et al.* (2015) that a high unblocking temperature magnetization is not present versus that of Dare *et al.* (2016), and Bono *et al.* (2018) that a high unblocking temperature component is present.

Herein, we use a combination of SEM and transmission electron microscopy (TEM) imagery, coupled with focused ion beam (FIB) tomography and crystal diffraction analyses to determine whether smaller magnetite grains predicted to be present in the Jack Hills cobbles on the basis of magnetic analyses (Tarduno & Cottrell 2013; Dare *et al.* 2016) can be imaged. Micromagnetic modelling was also

Downloaded from https://academic.oup.com/gji/article-abstract/216/1/598/5144769 by Univ of Rochester Library user on 23 November 2018

performed to determine whether the submicrometre magnetites observed that are above the size threshold for SD magnetite are expected to behave as stable, single vortex state PSD grains. We note that very small submicrometre grains in the PSD or SD states are capable of preserving primary magnetizations over billions of years (Butler & Banerjee 1975; Dunlop & Özdemir 1997; Nagy *et al.* 2017). This temporal recording fidelity is required for assessing whether bulk Jack Hills sediments yield useful constraints on magnetization ages. The results of this study are the first direct microscopic confirmation, using TEM diffraction analysis and energy dispersive spectroscopy, of the presence of submicrometre magnetite in the Jack Hills quartzite conglomerate. Micromagnetic modelling supports the interpretation that magnetite grains consistent with a single vortex PSD state behaviour are present.

2 MATERIALS AND METHODS

Jack Hills quartzite cobble samples studied here are from the collections detailed by Tarduno & Cottrell (2013) and Bono *et al.* (2018). Billets ∼2 cm thick were cut from the centre of select cobbles and polished ∼30 mm thick sections were prepared for light and electron microscopic study (further details on sample preparation can be found in Dare *et al.* 2016). Microscope slides were initially polished with alumina with a final polish using 0.05 mm colloidal silica. Prior to SEM study, samples were evaporatively coated with 10–15 nm of carbon to enhance conductivity and reduce surface charging.

Polished thin sections were first examined using a Zeiss Auriga SEM at the University of Rochester, using secondary and backscattered electron detectors (SE2 and BSD, respectively) to test for the presence of submicrometre iron oxide detrital grains. Qualitative compositions were determined using EDS (accelerating voltages were typically 10 keV). Care was taken to avoid iron oxides along cracks, since these may have formed as secondary minerals during alteration/weathering of the cobble after deposition. Relatively large (>1 mm) iron oxides and other oxide phases were easily observed, but because these have been previously studied in depth by Dare *et al.* (2016), they were not further documented for the purposes of this study. Instead our focus was on submicrometre grains, which were also observed, with composition constrained by EDS analysis. After identification of an iron oxide grain, the exposed dimensions of the grain were measured using the open source software ImageJ (Table 1).

To further characterize the composition of the iron oxide grains, TEM studies were performed. TEM samples were prepared from identified submicrometre iron oxide grains using FIB (equipped within the Zeiss Auriga SEM at the University of Rochester) milling to expose electron transparent lamellae containing the target grain (using methods similar to those described by Gianuzzi & Stevie 1999; Mayer *et al.* 2007). Sample lamellas were removed from microscope slides using a tungsten probe and attached to copper TEM grids with platinum. Sample lamellae (typically 10–20 μm in length) were thinned to electron transparency (< 100 nm). After thinning, additional EDS were collected to confirm the composition of iron oxide. In the TEM, high-resolution cross-sectional images and EDS measurements were collected from the target iron oxide grain. Electron diffraction patterns were also collected to identify the crystallinity of the grain used to determine composition.

One other submicrometre detrital iron oxide grain from cobble JC43 was selected for micromagnetic modelling to characterize the domain state of these grains. Here, the FIB was used to expose the cross-section of a target grain and then progressively remove 10–20 nm thick slices of the cross-sectional wall, analogous to the FIB-nanotomography method described by Einsle *et al.* (2016). Adjacent to the target grain a fiducial was milled into the platinum. One edge of the volume intended to be tomographically milled was initially exposed through FIB milling at high power (1 nA). Afterwards, low power milling (10 pA, ∼100 s intervals) progressively advanced through the target volume. Milling was observed with SE imaging with an accelerating voltage of 5 keV. After each mill, the exposed cross-section was imaged with SEs at 5 keV at fixed magnification intervals (30 and 100 kX). At each step, SE images were collected under repeated imaging conditions at 5 keV. In addition to cross-section images, a plan view (top down) image was collected between each milling interval. Using the fiducial mark applied prior to the start of milling, the thickness of material removed can be estimated (on average, ∼10.5 μm per milling interval). Throughout the procedure, the position and angle of the sample stage was recorded to ensure that images were collected from the same angle, distance and magnification.

After completion of the FIB-tomography milling, the following procedure was used to prepare the micromagnetic modelling mesh. High magnification (100 kX) SE images were used to define the extent of the target grain. Images were aligned using fixed reference features common to all images. In one instance, the image was collected at a slightly different magnification (100.21 kX) and required resizing. The collected images have a resolution of 1.11 nm pixel^{-1}. Since the SEs comprising the image were generated within an interaction volume extending into the exposed cross-section, the transition between target grain edge and surrounding matrix was not defined by a sharp transition but instead a gradient between light (target iron oxide) and dark pixels (surrounding silica matrix). To define the grain edge (segmentation), an iterative procedure of image threshold binarization and small pixel radius Gaussian blurring was applied identically to each milling interval cross-sectional image. The maximum cross-sectional dimensions were recorded after the grain edges were defined.

The resulting segmented images were segmented into binary images for each slice using a combination of ImageJ and Adobe Photoshop and exported for mesh generation. 3-D models and meshes were prepared from TIFF image stacks using MEshRRILL (Ó Conbhuí and Williams, personal communication, 2017). Micromagnetic modelling with MERRILL (Micromagnetic Earth Related Robust Interpreted Language Laboratory) was used to simulate the magnetic domain structure for the observed iron oxide. MERRILL employs a finite-element modelling method to simulate the local energy minima (LEM) for the given grain geometry (Ó Conbhuí *et al.* 2018). The procedure for finding the LEM of the target grain starting with randomized initial magnetizations for each node is similar to the one employed by Nagy *et al.* (2017) and is detailed in Ó Conbhuí *et al.* (2018).

3 RESULTS

Using SEM, 57 submm iron oxides (Table 1, and Tables S1 and S2, Supporting Information) were identified from two Jack Hills quartzite cobble sample microscope slides (JC43, n=43, and JC57, n=14). The grains are not homogeneously distributed. Instead, the iron oxides are found in clusters, likely due to isolated deposition layers carrying the grains, which may (or may not) be revealed during sample preparation (representative photographs of quartzite cobble sampling, Figs 2a and b). This further highlights the need

Downloaded from https://academic.oup.com/gji/article-abstract/216/1/598/5144769 by Univ of Rochester Library user on 23 November 2018

Table 1. Summary of detrital iron oxide dimensions.

	N	Minimum dimension (nm)	Maximum dimension (nm)	Median length (nm)	Length 95 per cent lower bound (nm)	Length 95 per cent upper bound (nm)	Median width (nm)	Width 95 per cent lower bound (nm)	Width 95 per cent upper bound (nm)	Median length/width	Length/width 95 per cent lower bound	Length/width 95 per cent upper bound
JC43	43	125	1960	744	259	1090	547	206	953	1.20	1.02	2.28
JC57	14	121	904	647	380	870	415	136	724	1.46	1.04	3.78
All	57	121	1960	703	266	1088	482	141	924	1.23	1.02	3.64

to carefully consider specimen volumes in palaeomagnetic analyses (cf. Dare *et al.* 2016). Identified grains range in size from ∼120 to ∼1200 nm, with a median exposed length of 703 nm (95 per cent lower bound: 266 nm; 95 per cent upper bound: 1088 nm) and width of 482 nm (95 per cent lower bound: 141 nm; 95 per cent upper bound: 924 nm) (representative examples in Fig. 1). While grains ranged in shape from equant (length/width ratio of 1.00) to highly elongated (length/width ratio of 4.20), most grains show rounded to subrounded morphologies consistent with a detrital origin.

Four submicrometre grains were selected for TEM study, prepared by FIB lamellae lift out. Electron diffraction images were analysed to identify which iron oxide (or iron) phase was sampled. One additional grain was selected for FIB nanotomography and micromagnetic modelling. In addition to submicrometre magnetite rare native iron (α-Fe, BCC phase) was observed (Fig. S1, Supporting Information). In total, the five magnetite samples studied in more detail are described below.

3.1 JC43, grain AE

In cobble sample JC43 (Figs 2a and b), the polished surface exposure of grain AE (Fig. 2c) measures 436 x 349 nm (length/width ratio of 1.25), from which a TEM lamellae was prepared (Fig. 2d) with a cross-sectional preserved thickness of 77 nm (Fig. 2e) measured in the TEM. Surface EDS (collected with the SEM, Fig. S2, Supporting Information) and transmission EDS confirm an iron oxide composition (Fig. 2f). Electron diffraction shows a rectangular arrangement consistent with a magnetite composition (Fig. 2g). The surrounding silica matrix has an amorphous composition (Fig. 2h). To identify phases using a measure unbiased by uncertainty in camera length calibration (Steeds & Morniroli 1992), we rely on two lines of evidence: the relative angle and ratio of d-spacing between lattice planes [$\{\bar{1}\bar{1}1\} - \{\bar{2}20\}$, angle: 92°, ratio: 1.72 (cf. 90°, 1.63, Weschler *et al.* 1984); Table S3, Supporting Information] are consistent with the reference values for magnetite.

3.2 JC57, grain AH1

The polished surface exposure of this grain measures 662 x 471 nm (length/width ratio of 1.41) with a cross-sectional preserved thickness of 354 nm (Fig. 3a). Surface EDS prior to FIB lamellae preparation (collected with the SEM) detected an iron oxide composition, however the signal could not be distinguished from the adjacent grain AH2 (below). Nevertheless, transmission EDS confirm an iron oxide composition (Fig. S2, Supporting Information). Electron diffraction shows a rectangular arrangement consistent with a magnetite composition (Fig. 3b). Camera length independent measures comparing the angle and ratio between lattice planes [$\{111\} - \{242\}$, angle: 86°, ratio: 2.63 (cf. 90°, 2.82, Weschler *et al.* 1984); Table S3, Supporting Information] support a magnetite identification.

3.3 JC57, grain AH2

The polished surface exposure of this grain measures 800 x 750 nm (length/width ratio of 1.07) with a cross-sectional preserved thickness of 636 nm (Fig. 3c). Transmission EDS confirm an iron oxide composition (Fig. S2, Supporting Information). Electron diffraction shows a rectangular arrangement consistent with a magnetite composition (Fig. 3d). The angle between lattice planes $\{\bar{1}\bar{1}1\} - \{\bar{2}20\}$ is 89.9° and the ratio between d-spacings is nearly identical to reference values for magnetite from Weschler *et al.* (1984).

3.4 JC57, grain AI

The polished surface exposure of this grain measures 783 x 475 nm (l/w ratio of 1.65) with a cross-sectional preserved thickness of 218 nm (Fig. 3e). Surface EDS (collected with the SEM) and transmission EDS confirm an iron oxide composition (Fig. S2, Supporting Information). Electron diffraction shows a rectangular arrangement consistent with a magnetite composition (Fig. 3f). Lattice planes $\{\bar{2}20\}$ and $\{353\}$ were observed: the angle between planes is 79° (cf. 77°), the ratio of d-spacings is 2.34 (cf. 2.31), with reference values for magnetite from Weschler *et al.* (1984).

3.5 JC43, grain BZ

JC43 grain BZ was selected for FIB tomography (Fig. 4a). After identification of the target grain and surface EDS data confirming an iron oxide composition were collected, the sample and surrounding region were coated in a 10 x 7 x ∼1 μm patch of gas-injected platinum was deposited to protect the surface and uppermost portion of the target grain from beam damage. In total, 29 mills were performed, of which 14 contained the target iron oxide grain. After every 4–5 intervals, energy dispersive spectra were collected, which confirmed the iron oxide composition. Grain dimensions are 148 x 125 x 100 nm with a roughly oblate shaped grain (Fig. 4b). Voxel dimensions of 1 x 1 x 11 nm were used to constrain the mesh generation, based on the measured image parameters. A smoothing factor of 16 was selected such that the resulting mesh model conformed to the observed shape of the iron oxide grain.

Micromagnetic simulations to minimize the energy state (i.e. identify domain state) of the grain were repeated 10 times from random initialization states, and seven additional times starting from a uniform magnetization state in different directions. The resulting micromagnetic simulations all suggest that the grain has a single vortex (pseudo-single) as a possible domain state (Fig. 4c). A single

Downloaded from https://academic.oup.com/gji/article-abstract/216/1/598/5144769 by Univ of Rochester Library user on 23 November 2018

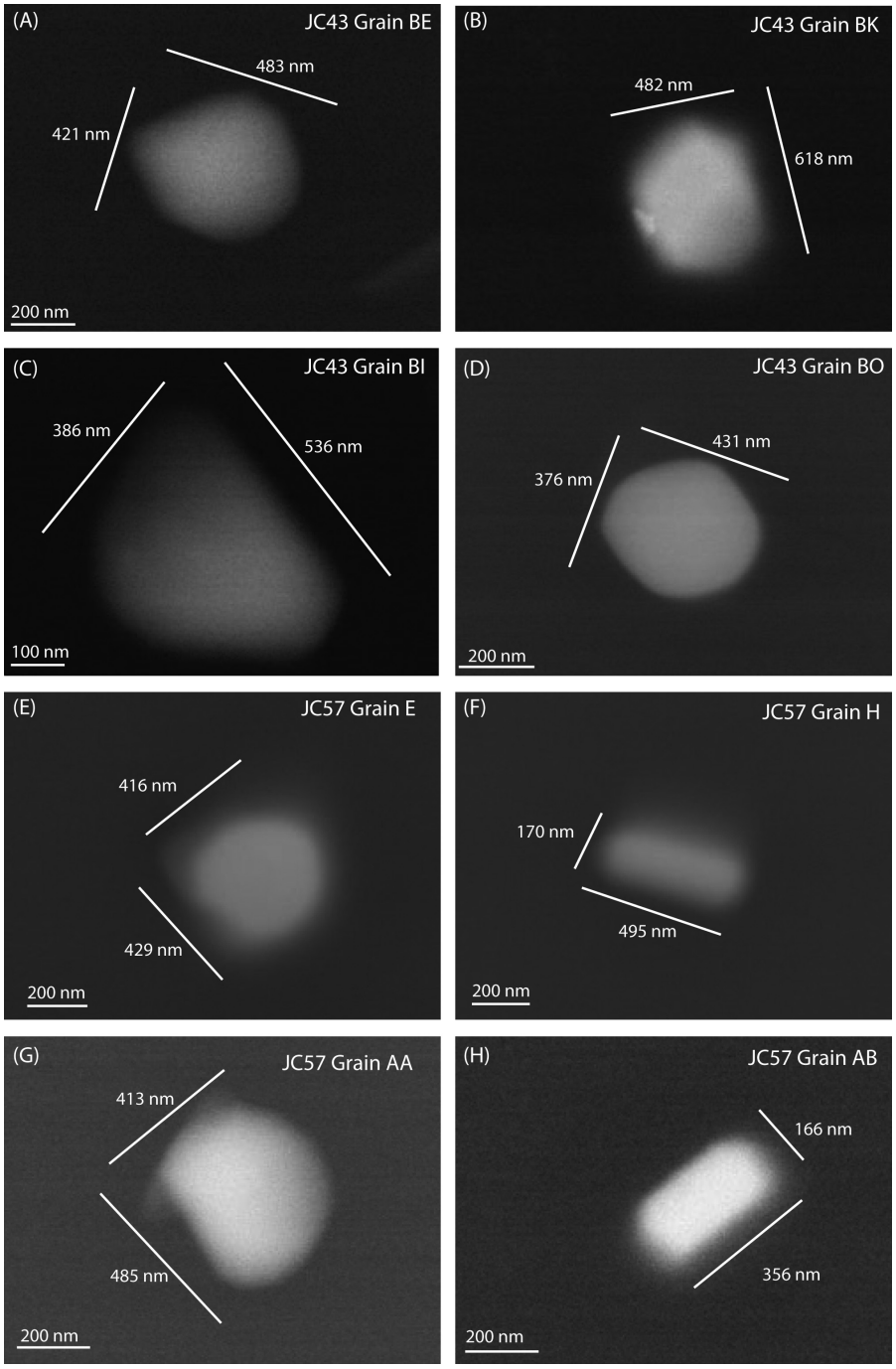

Figure 1. Representative SEM backscattered electron micrographs of submicrometre detrital iron oxides. (a)–(d) Jack Hills cobble JC43; and (e)–(h) Jack Hills cobble JC57.

vortex configuration for a magnetite grain of the approximate size observed in the target is consistent with the numerical simulations of Nagy *et al.* (2017) and Roberts *et al.* (2017), which have they interpret as robust magnetic carriers which can retain magnetizations on billion-year timescales.

4 DISCUSSION

Previous palaeomagnetic studies of Jack Hills conglomerate quartzite cobbles documented a characteristic remanent magnetization at high unblocking temperatures (Tarduno & Cottrell

Downloaded from https://academic.oup.com/gji/article-abstract/216/1/598/5144769 by Univ of Rochester Library user on 23 November 2018

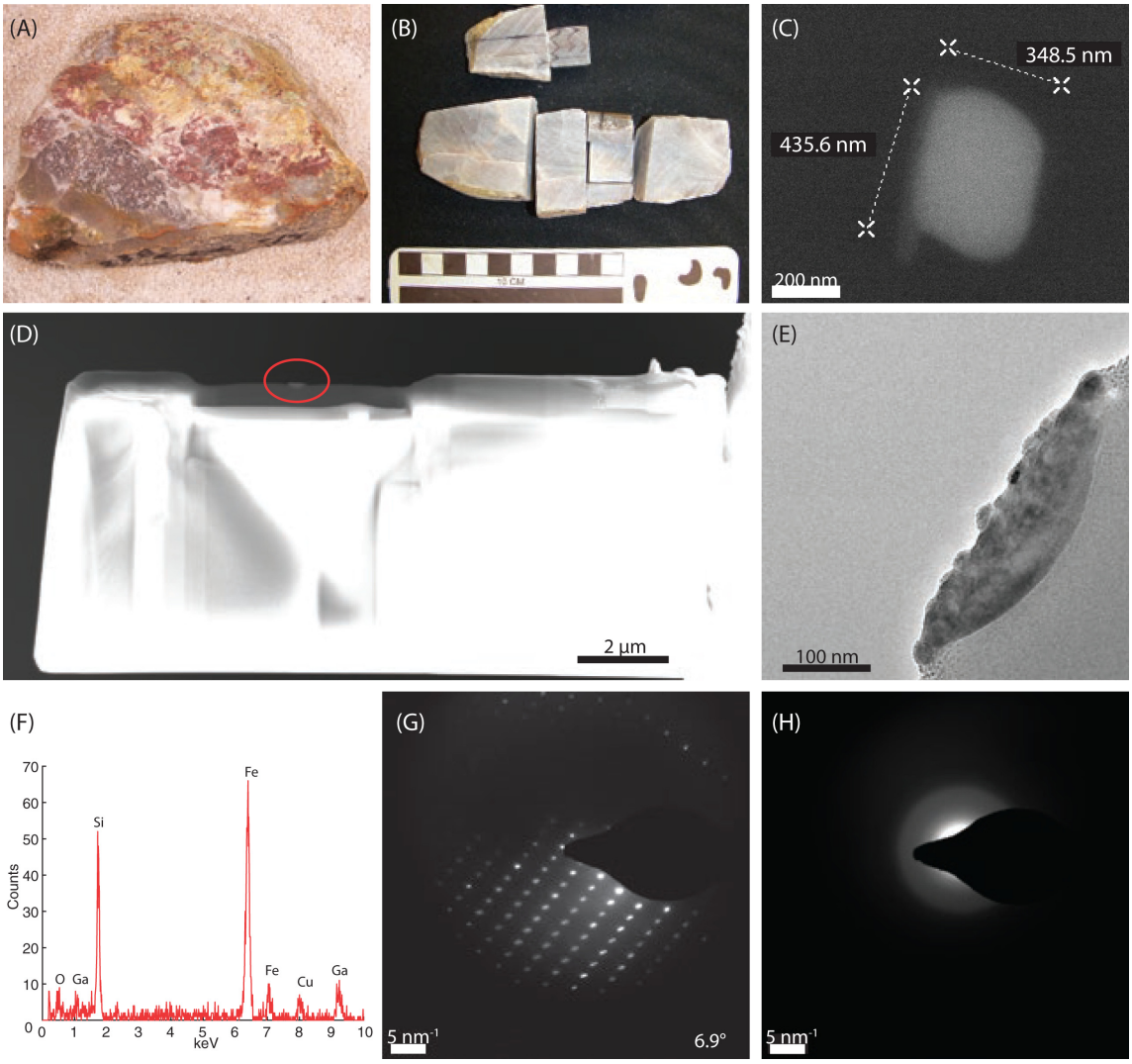

Figure 2. Focused Ion Beam (FIB) lift out of detrital magnetite grain from Jack Hills cobble JC43. (a) Jack Hills cobble JC43 prior to subsampling. (b) Cobble JC43 interior. (c) Backscattered electron micrograph of detrital magnetite grain AE. (d) FIB-TEM lamellae cross-section containing grain AE (red circle). (e) Transmission electron micrograph (bright field emission) of grain AE in cross-section. (f) Energy dispersive X-ray spectra of grain AE confirming iron oxide composition. (g) Electron diffraction pattern of grain AE confirming magnetite composition. (h) Electron diffraction pattern of surrounding silica matrix.

2013; Tarduno *et al.* 2015; Dare *et al.* 2016). The high unblocking temperatures (>500–580 °C) are consistent with presence of SD to PSD magnetite. Previous microscopic study (Dare *et al.* 2016) documented magnetite in Jack Hills quartzite cobbles. However, that study was a broad survey of magnetic carriers and led to the documentation on only micrometre-scale magnetites which are likely in the MD magnetic state. Here, our observations using electron microscopy coupled with compositional analysis (EDS, electron diffraction), provides the first imaging of SD to PSD size magnetite in Jack Hills quartzite cobbles.

The preservation of a characteristic detrital remanence for ∼3 billion years is consistent with predictions of magnetic relaxation theory for SD grains carrying a thermoremanent magnetization (TRM). Specifically, under Néel (1955) theory, the thermal relaxation time (τ) can be described as follows (Dunlop & Özdemir 1997):

$$\frac{1}{\tau} = \frac{1}{\tau_0}\exp\left[-\frac{\mu_0 V M_s H_K}{2kT}\left(1-\frac{|H_0|}{H_K}\right)^2\right]$$

with μ_0: permeability of free space, V: grain volume, M_S: spontaneous magnetization, H_K: microscopic coercive force, k: Boltzmann's constant, T: temperature, H_0: applied field and τ_0: interval between thermal excitations. Equant magnetite grains ∼20–80 nm in size can have τ values of billions of years. Larger elongated grains are capable of maintaining SD-like behaviour due to shape

Downloaded from https://academic.oup.com/gji/article-abstract/216/1/598/5144769 by Univ of Rochester Library user on 23 November 2018

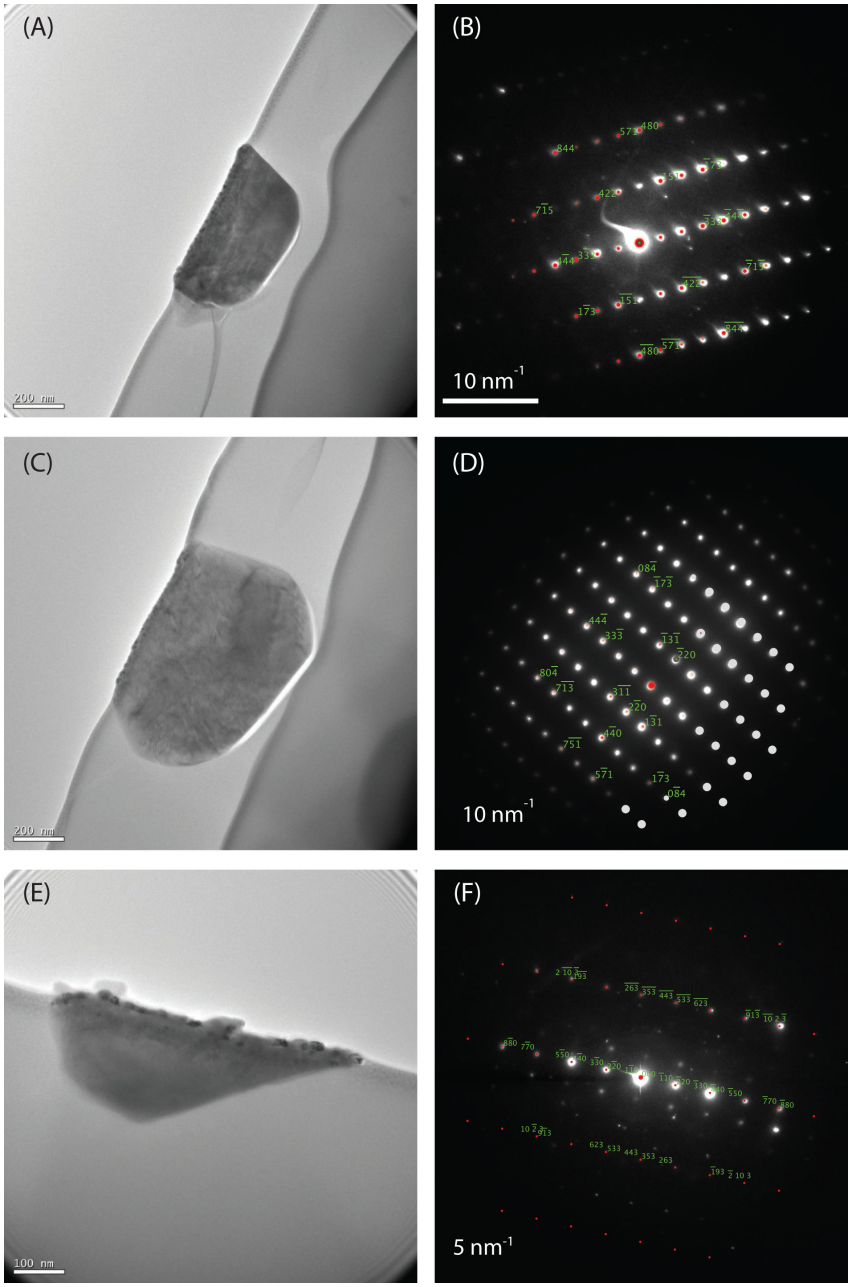

Figure 3. (a), (c) and (e) TEM micrographs and (b), (d) and (f) corresponding electron diffraction patterns of detrital magnetite grains from Jack Hills cobble JC57. (a) and (b) grain AH1; (c) and (d) grain AH2 and (e) and (f) grain AI.

anisotropy preventing the formation of domain walls (Butler & Banerjee 1975).

The presence of magnetite with sizes greater than the SD threshold does not preclude the ability to retain magnetizations on billion year timescales above blocking temperatures approaching the Curie temperature of magnetite (580 °C). Equant magnetite greater than 80 nm in size will form magnetic subdomains. In large ($>> 1\ \mu$m) grains, referred to as MD grains, the recovery of a TRM becomes problematic because of the multiple LEMs which can result in a new equilibration of domain walls (Dunlop & Xu 1994). For this reason, MD magnetic carriers are often considered unsuitable for recording ancient magnetizations.

However, between the threshold where an SD grain partitions into two domains and true MD grains fall PSD grains, with equidimensional sizes ranging between 80 and >1000 nm (Dunlop & Özdemir 1997). Neither SD nor MD theory adequately describes the behaviour of PSD grains, nevertheless PSD grains are ubiquitous magnetic particles in rocks, and in many cases carry the majority of the magnetic remanence (Day *et al.* 1977). Near the SD–PSD transition zone, PSD grains can have single-vortex domain states

Downloaded from https://academic.oup.com/gji/article-abstract/216/1/598/5144769 by Univ of Rochester Library user on 23 November 2018

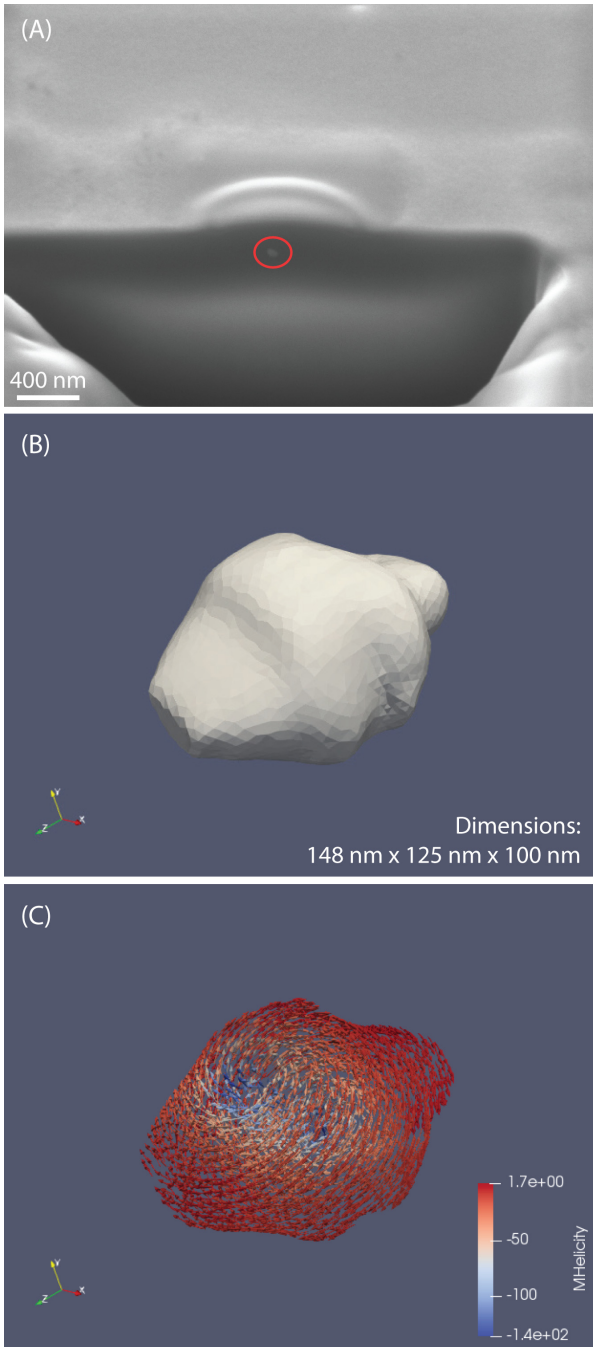

Figure 4. Focused Ion Beam (FIB) tomography and micromagnetic model of Jack Hills magnetic carrier. (a) Scanning electron micrograph showing cross-section of Jack Hills cobble magnetic carrier (red circle), exposed using an FIB at the University of Rochester. Target grain was subsequently thinned using the FIB, with SEM micrographs captured approximately every 10–20 nm. (b) From FIB tomographic image stack a 3-D model was developed using MEshRILL (Ó Conbhuí and Williams, personal communication, 2017). (c) Resulting 3-D model was used as the basis for a micromagnetic model using MERRILL (Ó Conbhuí *et al.* 2018) following the protocol of Nagy *et al.* (2017). Single vortex pattern demonstrates pseudo-single-domain structure which stably retains magnetizations over billion-year timescales.

which behave like SD magnetic carriers, above this size range the PSD grains can express complex multivortex and MD-like configurations (Enkin & Williams 1994). Recent direct observations (Almeida *et al.* 2016) and micromagnetic modelling (Nagy *et al.* 2017; Roberts *et al.* 2017) of PSD (titano)magnetite suggests that these grains are exceedingly stable on billion-year timescales and can also act as ideal magnetic recorders. The $<1\ \mu$m grains observed in the Jack Hills quartzite cobbles are typically slightly elongated in shape compared to those simulated by Nagy *et al.* (2017). Thus, it would be expected that their modelled relaxation times represent minimum values for the PSD grains of this study.

Here, the observation of submicrometre (i.e. SD and PSD) magnetite grains in Jack Hills quartzite cobbles supports the prior interpretations of a high unblocking temperature characteristic remanence carrier (Fig. 5). While a formal theory on the transition between PSD and MD domain states remains to be developed, existing theory and observations (Nagy *et al.* 2017); Almeida *et al.* (2016) demonstrate that magnetic carriers like the ones seen in the Jack Hills are capable of retaining remanence magnetizations for billions of years, consistent with prior palaeomagnetic interpretations (Tarduno & Cottrell 2013; Tarduno *et al.* 2015; Dare *et al.* 2016; Bono *et al.* 2018). The absence of metastable flower state configurations in the micromagnetic simulations exclude the potential for a viscous transformation which could mimic a primary high unblocking temperature magnetization (de Groot *et al.* 2014; Fabian & Shcherbakov 2018).

The presence of submicrometre magnetite is not uniform throughout all of the samples investigated in this study. Instead, individual slide preparations were observed to be mostly (entirely) absent of submicrometre magnetite, wherein other slides submicrometre iron oxides were ubiquitous. The absence or presence of submicrometre iron oxides likely reflects differences in deposition of iron oxides. Variations in input volume could record changes in environment or provenance of the sediments which comprise the quartzite prior to metamorphism.

The presence of rare native iron which is likely detrital in origin (due to the subrounded shape of the grain) is consistent with formation and transport in an anoxic environment of the Archean (e.g. Farquhar *et al.* 2000). The oldest previous report of preserved native iron has been from Proterozoic sediments and interpreted as ejecta from a pre-1.6 Ga impact (Abbott *et al.* 2006; Chandra *et al.* 2010). The Jack Hills occurrence, if confirmed (we note it is currently defined by a single grain), would extend this record back in time by ca. 1.4 billion years. The provenance of native iron in the Jack Hills is unknown, but it could have a meteoritic, impact ejecta or ultramafic source. The grain's preservation through to the present can be explained due to the protective shielding provided by the surrounding silica matrix of the quartzite. Preservation of a native iron phase reinforces that submicrometre iron and iron oxide phases can see through metamorphic alteration events if well protected.

The SD–PSD magnetite in the Jack Hills cobbles identified here should record high unblocking temperatures. On the basis of the average number of grains seen in our SEM studies, we estimate that $\mathcal{O} \sim 10^7$–10^8 SD/PSD magnetite particles could be present in the 3–6 cm^3 palaeomagnetic samples examined. This should be sufficient to record the high unblocking temperature magnetization, even if the detrital/post-depositional remanence process was inefficient. For completeness, we note that the presence of larger magnetite grains studied by Dare *et al.* (2016), together with the known thermal overprint, raises the question of the importance of 'pTRM tails', the unblocking of MD particles at high temperatures (e.g. Shcherbakova *et al.* 2000). However, in this case we should expect the pTRM

Downloaded from https://academic.oup.com/gji/article-abstract/216/1/598/5144769 by Univ of Rochester Library user on 23 November 2018

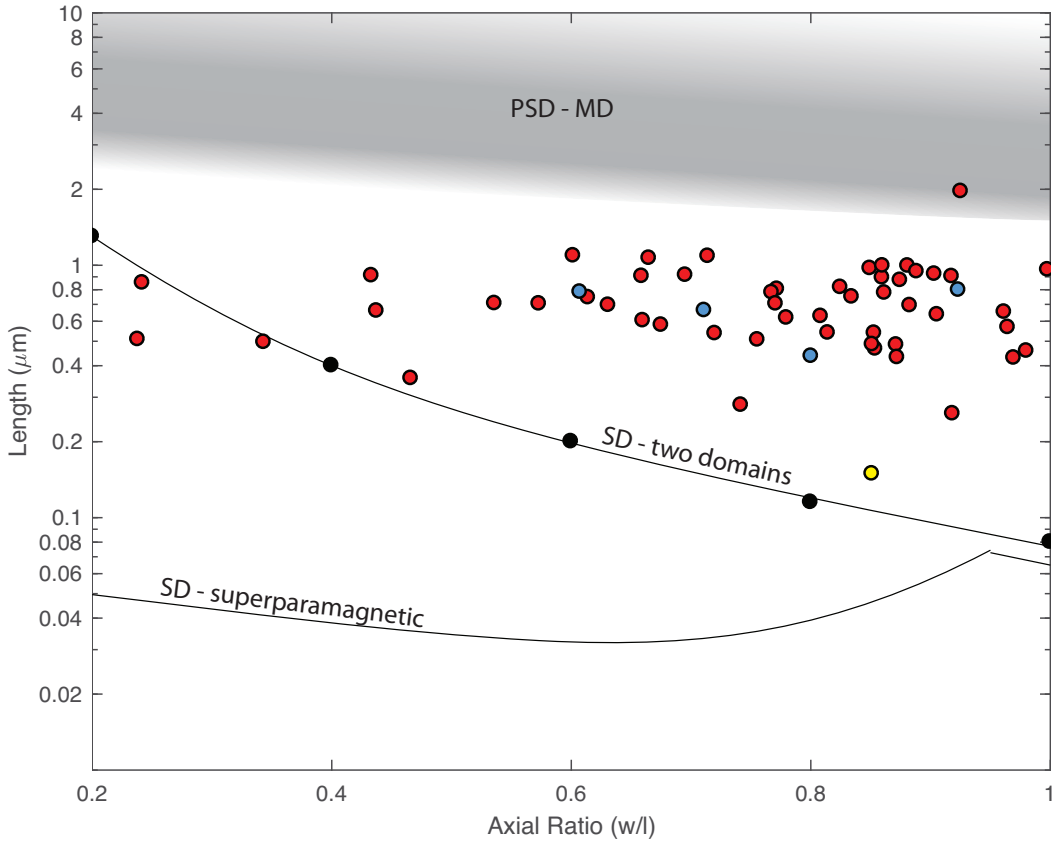

Figure 5. Summary of exposed surface dimensions of detrital iron oxides, shown relative to domain transition zones for magnetite. Red points: grains imaged with SEM only; blue points: grains characterized with TEM; and yellow point: grain simulated with micromagnetic modelling software MERRILL. The majority of the oxides fall within the pseudo-single-domain grain size range and trend towards the single-domain transition, consistent with a magnetic carrier with high unblocking temperatures (~550–580 °C) and stable remanence preservation on billion-year timescales. Single-domain transition from Butler and Banerjee (1975). Grey shaded region shows approximate pseudo-single (single vortex) to multidomain transition zone.

tail to carry an overprint direction equivalent to that seen at lower unblocking temperatures. Bono *et al.* (2018) conducted a detailed search for this direction and it is not present in the Jack Hills high unblocking temperature data, indicating that the pTRM tails are not significant.

The presence of SD and single vortex PSD grains support the interpretation that the failure of Weiss *et al.* (2015) to define such a component in most of their analyses relates to inferior data quality. Dare *et al.* (2016) provide a detailed analysis, and guidelines for high-resolution analyses. Finally, we note that Weiss *et al.* (2018) focus on secondary magnetic particles in JH zircons and renew calls for remagnetization. Secondary oxides were recognized by Tarduno *et al.* (2015) and their role as important carriers of characteristic remanence was excluded on the basis of a microconglomerate test on samples from the Discovery site.

5 CONCLUSIONS

We report for the first time direct observations of detrital, SD and single-vortex PSD domain magnetite in JH quartzite cobbles. This form of magnetite is suitable for retaining characteristic remanence magnetizations which unblock at temperatures which exceed the metamorphic reheating temperature for the Jack Hills. Furthermore, SD and PSD magnetite is ideal for retaining magnetizations on billion year timescales.

The SD–PSD magnetite grains imaged here confirm the findings of Tarduno and Cottrell (2013) and Dare *et al.* (2016), who predicted their presence on the basis of thermal demagnetization data, electron microscopy of larger detrital magnetite grains and inferences about sedimentary grain distributions. The failure of some groups (e.g., Weiss *et al.* 2015) to define high unblocking temperature magnetizations in analyses of JH quartzite cobbles, which demonstrably contain SD–PSD magnetite, points to data with limited resolution (cf. Dare *et al.* 2016).

The presence of SD–PSD detrital grains strengthens the conclusion that the JH quartzite cobbles retain an Archean age magnetization at high unblocking temperatures and that, overall, the JH metasediments have not been completely remagnetized. This in turn supports the conclusion that zircons of the Discovery Site (Tarduno *et al.* 2015) preserve primary records that attest to the presence of a Hadean geodynamo.

ACKNOWLEDGEMENTS

Matthew S. Dare and Tim O'Brien for sample preparation and SEM work. Ralph Wiegandt and Brian McIntyre for FIB work. Padraig Ó Conbhuí provided MEshRRILL software which generated FEM

Downloaded from https://academic.oup.com/gji/article-abstract/216/1/598/5144769 by Univ of Rochester Library user on 23 November 2018

meshes of magnetite grains. We are grateful for the helpful discussions with Les Nagy and Wyn Williams on the interpretation of micromagnetic models, and with Karl Dawson on the interpretation of TEM electron diffraction images. We would like to thank Karl Fabian and an anonymous reviewer for their helpful comments. This work was supported by NSF grant EAR 1656348 to John A. Tarduno.

REFERENCES

Abbott, D., Mazumder, R. & Breger, D., 2006. Native iron in the Chaibasa Shales: result of a pre 1.6 Ga impact?, in *37th Annual Lunar and Planetary Science Conference,* Abstract 1899, Lunar and Planetary Institute.

Almeida, T.P., Muxworthy, A.R., Kovács, A., Williams, W., Brown, P.D. & Dunin-Borkowski, R.E., 2016. Direct visualization of the thermomagnetic behavior of pseudo-single-domain magnetite particles, *Sci. Adv.,* **2**(4), e1501801.

Bono, R.K. & Tarduno, J.A., 2015. A stable Ediacaran Earth recorded by single silicate crystals of the ca. 565 Ma Sept-Îles Intrusion, *Geology,* **43**(2), 131–134.

Bono, R.K., Tarduno, J.A. & Cottrell, R.D., 2016. Comment on: Pervasive remagnetization of detrital zircon host rocks in the Jack Hills, Western Australia and implications for records of the early dynamo, by Weiss et al. (2015), *Earth planet. Sci. Lett.,* **450,** 406–408.

Bono, R.K., Tarduno, J.A., Dare, M.S., Mitra, G. & Cottrell, R.D., 2018. Cluster analysis on a sphere: application to magnetizations from metasediments of the Jack Hills, Western Australia, *Earth planet. Sci. Lett.,* **484,** 67–80.

Butler, R.F. & Banerjee, S.K., 1975. Theoretical single-domain grain size range in magnetite and titanomagnetite, *J. geophys. Res.,* **80**(29), 4049–4058.

Chandra, U., Sharma, P., Parthasarathy, G. & Sreedhar, B., 2010. ^{57}Fe Mössbauer spectroscopy and electrical resistivity studies on naturally occurring native iron under high pressures up to 9.1 Ga, *Am. Mineral.,* **95**(5–6), 870–875.

Cottrell, R.D. & Tarduno, J.A., 1999. Geomagnetic paleointensity derived from single plagioclase crystals, *Earth planet. Sci. Lett.,* **169**(1), 1–5.

Cottrell, R.D. & Tarduno, J.A., 2000. In search of high-fidelity geomagnetic paleointensities: a comparison of single plagioclase crystal and whole rock Thellier-Thellier analyses, *J. geophys. Res.,* **105,** 23579–23594.

Cottrell, R.D., Tarduno, J.A., Bono, R.K., Dare, M.S. & Mitra, G., 2016. The inverse microconglomerate test: further evidence for the preservation of Hadean magnetizations in metasediments of the Jack Hills, Western Australia, *Geophys. Res. Lett.,* **43**(9), 4215–4220.

Cottrell, R.D., Tarduno, J.A. & Roberts, J., 2008. The Kiaman Reversed Polarity Superchron at Kiama: toward a field strength estimate based on single silicate crystals, *Phys. Earth planet. Inter.,* **169**(1), 49–58.

Dare, M.S., Tarduno, J.A., Bono, R.K., Cottrell, R.D., Beard, J.S. & Kodama, K.P., 2016. Detrital magnetite and chromite in Jack Hills quartzite cobbles: further evidence for the preservation of primary magnetizations and new insights into sediment provenance, *Earth planet. Sci. Lett.,* **451,** 298–314.

Day, R., Fuller, M. & Schmidt, V.A., 1977. Hysteresis properties of titanomagnetites: grain-size and compositional dependence, *Phys. Earth planet. Inter.,* **13**(4), 260–267.

de Groot, L.V., Fabian, K., Bakelaar, I.A. & Dekkers, M.J., 2014. Magnetic force microscopy reveals meta-stable magnetic domain states that prevent reliable absolute palaeointensity experiments, *Nat. Commun.,* **5,** 4548.

Dunlop, D.J., 2002. Theory and application of the day plot (M_{RS}/M_S versus H_{CR}/H_C) 1. theoretical curves and tests using titanomagnetite data, *J. geophys. Res.,* **107** .

Dunlop, D.J. & Xu, S., 1994. Theory of partial thermoremanent magnetization in multidomain grains: 1. Repeated identical barriers to wall motion (single microcoercivity), *J. geophys. Res.,* **99,** 9005–9023.

Dunlop, D.J. & Özdemir, O., 1997. *Rock Magnetism: Fundamentals and Frontiers,* Cambridge University Press.

Einsle, J.F. *et al.*, 2016. Multi-scale 3-dimensional characterisation of iron particles in dusty olivine: implications for paleomagnetism of chondritic meteorites, *Am. Mineral.,* **101**(9), 2070–2084.

Enkin, R.J. & Williams, W., 1994. Three-dimensional micromagnetic analysis of stability in fine magnetic grains, *J. geophys. Res.,* **99,** 611–618.

Evans, D.A.D., 2018. RESEARCH FOCUS: probing the complexities of magnetism in zircons from Jack Hills, Australia, *Geology,* **46**(5), 479–480.

Fabian, K. & Shcherbakov, V.P., 2018. Energy barriers in three-dimensional micromagnetic models and the physics of thermoviscous magnetization, *J. geophys. Res.,* **215,** 314–324.

Farquhar, J., Bao, H. & Thiemens, M., 2000. Atmospheric influence of Earth's earliest sulfur cycle, *Science,* **289,** 756–758.

Feinberg, J.M., Scott, G.R., Renne, P.R. & Wenk, H.-R., 2005. Exsolved magnetite inclusions in silicates: features determining their remanence behavior, *Geology,* **33**(6), 513–516.

Giannuzzi, L.A. & Stevie, F.A., 1999. A review of focused ion beam milling techniques for TEM specimen preparation, *Micron,* **30**(3), 197–204.

Koppers, A., Minnett, R.C., Tauxe, L., Constable, C. & Donadini, F., 2008. Managing rock and paleomagnetic data flow with the MagIC Database: from measurement and analysis to comprehensive archive and visualization, *Eos Trans. AGU,* **89**(53), GP11A–0708, Fall Meet. Suppl. Abstract.

Mayer, J., Giannuzzi, L.A., Kamino, T. & Michael, J., 2007. TEM Sample preparation and FIB-induced damage, *MRS Bull.,* **32**(5), 400–407.

Muxworthy, A.R., Evans, M.E., Scourfield, S.J. & King, J.G., 2013. Paleointensity results from the late-Archaean Modipe gabbro of Botswana, *Geochem. Geophys. Geosyst.,* **14**(7), 2198–2205.

Nagy, L., Williams, W., Muxworthy, A.R., Fabian, K., Almeida, T.P., Conbhuí, P.O. & Shcherbakov, V.P., 2017. Stability of equidimensional pseudo-single-domain magnetite over billion-year timescales, *Proc. Natl. Acad. Sci.* **114**(39), 10356–10360.

Néel, L., 1955. Some theoretical aspects of rock-magnetism, *Adv. Phys.,* **4**(14), 191–243.

Rasmussen, B., Fletcher, I.R., Muhling, J.R., Gregory, C.J. & Wilde, S.A., 2011. Metamorphic replacement of mineral inclusions in detrital zircon from Jack Hills, Australia: implications for the Hadean Earth, *Geology,* **39**(12), 1143–1146.

Roberts, A.P. *et al.*, 2017. Resolving the origin of pseudo-single domain magnetic behavior, *J. geophys. Res.,* **122**(12), 9534–9558.

Selkin, P.A., Gee, J.S., Meurer, W.P. & Hemming, S.R., 2008. Paleointensity record from the 2.7 Ga Stillwater complex, Montana, *Geochem. Geophys. Geosyst.,* **9**(12), Q12023.

Shcherbakova, V.V., Shcherbakov, V.P. & Heider, F., 2000. Properties of partial thermoremanent magnetization in pseudosingle domain and multidomain magnetite grains, *J. geophys. Res.,* **105,** 767–781.

Smirnov, A.V., Evans, D.A.D., Ernst, R.E., Söderlund, U. & Li, Z.-X., 2013. Trading partners: tectonic ancestry of southern Africa and Western Australia, in Archean supercratons Vaalbara and Zimgarn, *Precambrian Res.* **224,** 11–22.

Smirnov, A.V., Tarduno, J.A. & Pisakin, B.N., 2003. Paleointensity of the early geodynamo (2.45 ga) as recorded in Karelia: a single-crystal approach, *Geology,* **31**(5), 415–418.

Steeds, J.W. & Morniroli, J.P., 1992. Selected area electron diffraction (SAED) and convergent beam electron diffraction (CBED), *Rev. Min. Geol.,* **27**(1), 37–84.

Tarduno, J., Bunge, H.-P., Sleep, N. & Hansen, U., 2009. The bent Hawaiian-Emperor hotspot track: inheriting the mantle wind, *Science,* **324**(5923), 50–53.

Tarduno, J.A., Blackman, E.G. & Mamajek, E.E., 2014. Detecting the oldest geodynamo and attendant shielding from the solar wind: implications for habitability, *Phys. Earth planet. Inter.,* **233,** 68–87.

Tarduno, J.A. & Cottrell, R.D., 2005. Dipole strength and variation of the time-averaged reversing and nonreversing geodynamo based on Thellier analyses of single plagioclase crystals, *J. geophys. Res.,* **110,** B11101.

Tarduno, J.A. & Cottrell, R.D., 2013. Signals from the ancient geodynamo: a paleomagnetic field test on the Jack Hills metaconglomerate, *Earth planet. Sci. Lett.,* **367,** 123–132.

Downloaded from https://academic.oup.com/gji/article-abstract/216/1/598/5144769 by Univ of Rochester Library user on 23 November 2018

Tarduno, J.A., Cottrell, R.D., Davis, W.J., Nimmo, F. & Bono, R.K., 2015. A Hadean to Paleoarchean geodynamo recorded by single zircon crystals, *Science,* **349**(6247), 521–524.

Tarduno, J.A., Cottrell, R.D. & Smirnov, A.V., 2002. The Cretaceous superchron geodynamo: observations near the tangent cylinder, *Proc. Natl. Acad. Sci.* **99**(22), 14020–14025.

Tarduno, J.A., Cottrell, R.D. & Smirnov, A.V., 2006. The paleomagnetism of single silicate crystals: Recording geomagnetic field strength during mixed polarity intervals, superchrons, and inner core growth, *Rev. Geophys.,* **44**(1), RG1002.

Tarduno, J.A., Cottrell, R.D., Watkeys, M.K. & Bauch, D., 2007. Geomagnetic field strength 3.2 billion years ago recorded by single silicate crystals, *Nature,* **446**(7136), 657–660.

Tarduno, J.A. & Smirnov, A.V., 2001. Stability of the Earth with respect to the spin axis for the last 130 million years, *Earth planet. Sci. Lett.,* **184**(2), 549–553.

Tarduno, J.A. *et al.*, 2010. Geodynamo, solar wind, and magnetopause 3.4 to 3.45 billion years ago, *Science,* **327**(5970), 1238–1240.

Wechsler, B.A., Lindsley, D.H. & Prewitt, C.T., 1984. Crystal structure and cation distribution in titanomagnetites (Fe3-xTixO4), *Am. Mineral.,* **69**(7), 754–770.

Weiss, B.P., *et al.*, 2018. Secondary magnetic inclusions in detrital zircons from the Jack Hills, Western Australia, and implications for the origin of the geodynamo, *Geology,* **46**(5), 427–430.

Weiss, B.P. *et al.*, 2015. Pervasive remagnetization of detrital zircon host rocks in the Jack Hills, Western Australia and implications for records of the early geodynamo, *Earth planet. Sci. Lett.,* **430,** 115–128.

Weiss, B.P. *et al.*, 2016. Reply to comment on "Pervasive remagnetization of detrital zircon host rocks in the Jack Hills, Western Australia and implications for records of the early dynamo", *Earth planet. Sci. Lett.,* **450,** 409–412.

Wilde, S.A., Valley, J.W., Peck, W.H. & Graham, C.M., 2001. Evidence from detrital zircons for the existence of continental crust and oceans on the Earth 4.4 Gyr ago, *Nature,* **409**(6817), 175–178.

Ó Conbhuí, P., Williams, W., Fabian, K., Ridley, P., Nagy, L. & Muxworthy, A.R., 2018. MERRILL: micromagnetic Earth related robust interpreted language laboratory, *Geochem. Geophys. Geosyst.,* **19**(4), 1080–1106.

SUPPORTING INFORMATION

Supplementary data are available at *GJI* online.

Figure S1. Transmission electron microscopy (TEM) study of sample JC43 grain BW interpreted to be detrital native iron (α-Fe, BCC phase). (a) Brightfield and (b) high angle annular dark field electron micrographs of the iron oxide grain. (c) Energy dispersive X-ray spectra showing an iron oxide composition surrounded by a silica matrix. Oxygen peak present in spectra due to contribution from the surrounding silica matrix. (d) Selected area electron diffraction suggesting a native iron composition for the isolated grain.

Figure S2. Energy dispersive X-ray spectra (EDS) showing composition of targeted submicrometre grains from Jack Hills quartzite conglomerate cobbles. Top: sample JC43 grain AE, EDS collected with an SEM at 10 keV of the grain while embedded in surrounding silica matrix (left) and with a TEM at 200 keV after FIB lamellae preparation of an electron transparent sample (right). Due to the small size of the grains relative to the total interacting volume generating X-rays, the signal from the iron oxide grain is overwhelmed by the surrounding silica matrix. Middle: sample JC57 grain AI, following the description of the top row. Bottom: sample JC57 grain AH1 and AH2, following the description of the top row, with the modification that since the grains were adjacent to each other ($< 1\ \mu$m separation) the interacting volume contains both grains.

Table S1. Dimensional measurements (exposed surface) of submicrometre iron oxide grains in sample JC43.

Table S2. Dimensional measurements (exposed surface) of submicrometre iron oxide grains in sample JC57.

Table S3. Electron diffraction phase identification.

Please note: Oxford University Press is not responsible for the content or functionality of any supporting materials supplied by the authors. Any queries (other than missing material) should be directed to the corresponding author for the article.

Downloaded from https://academic.oup.com/gji/article-abstract/216/1/598/5144769 by Univ of Rochester Library user on 23 November 2018